IEEE Access
Multidisciplinary | Rapid Review | Open Access Journal

Received May 24, 2022, accepted June 6, 2022, date of publication June 14, 2022, date of current version June 17, 2022.

Digital Object Identifier 10.1109/ACCESS.2022.3183133

Enhanced Efficiency of Direct-Drive Switched Reluctance Motor With Reconfigurable Winding Topology

PENG YANG[1,2], WEI SHI[3], YUE QIU[4], BINGCHU LI[3], (Member, IEEE), AND YI GAN[3]

[1]School of Aeronautics and Astronautics, Shanghai Jiao Tong University, Minhang, Shanghai 200240, China
[2]Shanghai Aircraft Design and Research Institute, COMAC, Pudong, Shanghai 201210, China
[3]School of Mechanical Engineering, University of Shanghai for Science and Technology, Yangpu, Shanghai 200433, China
[4]CRRC Industrial Research Institute, Qingdao, Shandong 266000, China

Corresponding author: Bingchu Li (bclicsu@sina.com)

This work was supported in part by the Key Project of National Natural Science Foundation of China under Grant 51935007, and in part by the National Natural Science Foundation of China under Grant 51975356.

ABSTRACT Direct-drive motors (DDM) serve a vital role in reducing assemble complexity of mechatronics system and improve operation efficiency. However, design of DDM for washing machine is difficult, DDM needs to generate high torque at ultra-low-speed during rinse and reach high speed during dehydration, while keeping high efficiency. This paper puts forward a direct-drive switched reluctance motor (DDSRM) with reconfigurable drive topology for washing machine, the connections between pole windings in one phase of DDSRM can be reconfigured according to rotational speed. Three winding topologies are proposed in this paper, which leads to different speed range, efficiency and winding current. Topology switching mechanism are given, efficiency of DDSRM under different topologies are compared to find optimal speed to switch topology. A fast power loss calculation model is built to analyze the influence of turn-on and turn-off angles on DDSRM efficiency under different topologies, an online switching angles optimization method that matches topology switching strategy is proposed. A 24/16 3-phase out-rotor DDSRM was used in experiment to verify the effectiveness of topology switching strategy and switching angels optimization method, the results showed that the speed range of DDSRM is extended, efficiency of DDSRM over wild speed range can be significantly improved. The DDSRM with reconfigurable winding topology is of great value in promoting direct-drive technology for house-hold appliances, hydraulic system and aerospace actuators.

INDEX TERMS Direct drive, switched reluctance motor, efficiency, drive topology, switching angle control.

I. INTRODUCTION

Direct-drive mechatronics system are favored by more consumers considering its high energy efficiency and compact structure [1], it has drawn attention in house-hold appliances, hydraulic system and aerospace actuators. Instead of conventional drive train with motor-reducer-belt-drum structure, motors in direct-drive washing machines connect with drum without reducer and belt, simple structure of new drive train leads to improved efficiency and reliability, however, it also brings some challenges for DDM. First, washing machines operate in rinse and dehydration modes alternatively, in which motor velocity and load differs significantly. The drum of washing machine with 5L capability rotates at speed of 50-60 rpm with load torque between 25 N·m - 30 N·m under rinse mode, while the velocity is 1500 rpm - 1800 rpm with output torque between 3 N·m - 5 N·m in dehydration mode. Without regulating output torque by reducer, the torque output capability of DDM is much bigger than conventional drive motor [2]. Second, the efficiency of DDM should be enhanced to increase economy in use and reduce carbon emissions. Third, maximum current and supply voltage is limited by household power supply system. The operation condition of washing machine drums requires DDM to have wide speed range with high efficiency while keeping large output capability at low speed, which made the design of direct-drive system of great challenge.

The motors commonly used in direct-drive washing machines include single-phase asynchronous motors, brushless DC motors, series-excited motors and switched

The associate editor coordinating the review of this manuscript and approving it for publication was Adamu Murtala Zungeru.

reluctance motors (SRM) [3]. SRMs have simple structure and low manufacturing cost, which has been widely used in aerospace, household appliances, ship transportation, and so on. Castano *et al.* discussed the advantages of SRM considering operating characteristics of washing machines [4], a comparison between SRM and single-phase two-speed asynchronous motor showed that energy consumption of SRM is only 47% of that for single-phase asynchronous motor. Asgara *et al.* introduced a 12/8 dual-stator SRM for washing machines, both finite element analysis and experiment have been carried out to verify the feasibility of SRM for washing machines [5].

Several researches has been conducted in order to increase the torque capability of SRM in aspects of both motor structure, winding structure and drive circuit. Li *et al.* proposed a 72/48 3-phase SRM with maximum output torque of 7000 N·m at rated speed 105 rpm [6]. Sun *et al.* compared SRM with different pole numbers, the results showed that 16/14 poles SRM had larger torque, less torque pulsation and higher efficiency than 16/10 poles SRM at low-speed range, this paper indicated that increasing rotor poles was an effective way to improve torque capability [7]. However, increasing pole pair numbers would complicate the manufacturing process. High rotor or stator number also means less conduction time in one phase, which may hinder increase of velocity for SRM. Outer-rotor structure has also been used to increase force arm length considering limited assembly space inside washing machine [8]. Fernandes *et al.* proposed an polyphase SRM with segmented rotor to improve torque capability, the commutation strategy was also modified where two adjacent phases are concurrently excited [9]. Davarpanah *et al.* proposed a novel 12/14 3-phase SRM with segmented C-core structure, as both teeth of stator pole in C-core structure generated positive torque [10], torque density of the new SRM was enhanced. In aspect of drive circuit, turn-off angle has been moved toward aligned position to increase torque capability of SRM, however, the backward turn-off angle may cause negative torque due to tail current. To solve tihs problem, Ahn proposed a novel passive boost power converter for single-phase SRM, a passive circuitis was added in the front-end of a conventional asymmetric converter to obtain high negative bias, which can suppress negative torque generation from the tail current and improve output power [11]. Ding proposed a novel boost converter to increase phase voltage through additional capacitor, faster-excitation and fast-demagnetization currents were obtained, the conduction anlge and output torque of SRM was enlarged with boosted converter [12]. Optimizing winding structure was also a promising approach to improve torque capability of SRM. Zhu *et al.* simultaneously excited two adjacent phase windings and found that the torque of SRM could be increased while torque pulsation being reduced [13]. Deng *et al.* proposed five different winding connections for six-phase SRM, different winding connections are compared in terms of torque characteristics, core losses and mutual inductance, and found an optimum winding configuration for SRM [14].

Speed range and opertaing efficiency of SRM are also of great improtance for washing machine. The main approach to improve speed range of SRM relies on diminution of winding inductance and increment of supply voltage [15]. The generation of power loss and efficiency optimization strategies for SRM have been investigated [16]–[18], the main approach to achieve high efficiency focus on maximizing average torque to current ratio within energy conversion loop. Switching angle optimization was also widely used to improve SRM efficiency. Xu *et al.* proposed an analytical calculation method for determining optimal switching angle based on a nonlinear inductance model [19], it improved SRM efficiency over wild speed range. Chen *et al.* proposed a novel method to search for optimal turn-on angle to minimize copper losses [20], the method performed well in case of start-up and sudden load change. Kittiratsatcha *et al.* introduced an artificial neural network to find optimal switching angles [21]. Then, contradiction arises between high torque capability, wild speed range and high efficiency. Considering requirement of washing machine, phase inductance should be designed at lower value in case back-EMF overlap the bus voltage at high speed; however, phase current needs to reach high value with low phase inductance to meet the demand of torque at low-speed, which may conflict with maximum allowable current in house-hold machine and reduce motor efficiency. At present, a common approach to balance torque capability and speed range is to increase power level of DDM, but cost and assembly space are increased.

In this paper, an outer-rotor SRM with high rotor and stator number is used for direct-drive washing machine, reconfigurable topology is proposed to achieve the balance between high torque at low-speed and wild speed range. Reconfigurable topology indicates the connecting topology for pole windings in one phase can be changed according to working condition. Three winding topologies, namely parallel topology, hybrid topology and serial topology, are proposed in this paper. The voltage for separate pole winding (VSPW) of SRM is different under diverse topologies, which lead to different efficiency, maximum speed and bus current. The topology can be switched according to working condition. The performance of different topology are compared at different working condition to establish reasonable topology switching rule. A fast power loss calculation model is built to analyze the influence of turn-on and turn-off angles on DDSRM efficiency under different topologies, turn-on and turn-on angle is optimized based on power loss calculation model. Hardware realization to switch winding topology is given in detail. A 24/16 3-phase out-rotor DDSRM is used in experiment to verify the effectiveness of winding reconfiguration method for DDSRM, the results show that SRM efficiency over wild speed range can be significantly improved. The innovations of this paper include:

1) A new concept of reconfigurablee winding topology for DDSRM is proposed, DDSRM can expand speed range while maintaining high torque at low speed with limitation on bus voltage and current, the implementation

of reconfigurable topology for SRM are also given.
2) The influence of winding topology on DDSRM efficiency is revealed, current waveforms under different topologies are compared, an online topology switching strategy is proposed.
3) A fast power loss calculation model is built, switching angle optimization method considering DDSRM efficiency is proposed based on fast power loss calculation model. The performance of DDSRM with topology switching strategy and switching angle optimal control is evaluated in both simulation and experiments.

The following chapters are arranged as follows: Chapter 2 introduces the principle of reconfigurable topology for DDSRM. The implementation of topology switching strategy is given in Chapter 3. In chapter 4, a fast power loss calculation model is proposed to build optimal switching angle control for DDSRM. The performance of DDSRM with reconfigurable topology is evaluated through experiments in Chapter 6. Chapter 7 concludes the whole paper.

II. INFLUENCE OF WINDING TOPOLOGY ON DDSRM PERFORMANCE

A. DESIGN CONSIDERATION OF DIRECT-DRIVE SRM

The DDSRM for washing machine connect with drum through rigidity transmission, operation speed and load capability of DDSRM need to be identical with drum. In washing mode, the drum change rotational direction frequently to bring washes into contact with washing-up liquid, DDSRM works at low speed with high load that made up of washes and massive water. In dehydration mode, much of water has been drain away, the washes are whirling with high velocity to shake off the rest, DDSRM needs to work at high speed. Besides, supply voltage and current of DDSRM are limited by safety requirements of washing machine, structure of DDSRM is limited by assembly space and cooling condition of washing machine. The design consideration for DDSRM used in washing machine are listed as follows:

1) The supply voltage for DDSRM drive is AC 220V, which would be transformed into DC voltage through rectifier.
2) Maximum bus current for DDSRM should not exceed 45 A.
3) Maximum output torque of DDSRM is bigger than 35 N·m at 50 rpm, while maximum continuous output torque should exceeds 25 N·m at 50 rpm.
4) Maximum speed of DDSRM should exceed 1400 rpm with 3 N·m load.
5) The diameter and length of DDSRM is smaller than 320 mm and 40 mm, respectively.

To acquire high torque density at low speed, outer-rotor SRM with high stator and rotor poles are generally used, a 3-phase 24/16 out-rotor SRM is designed and used as direct-drive motor for washing machine in this paper, the structure of DDSRM has been optimized thourgh

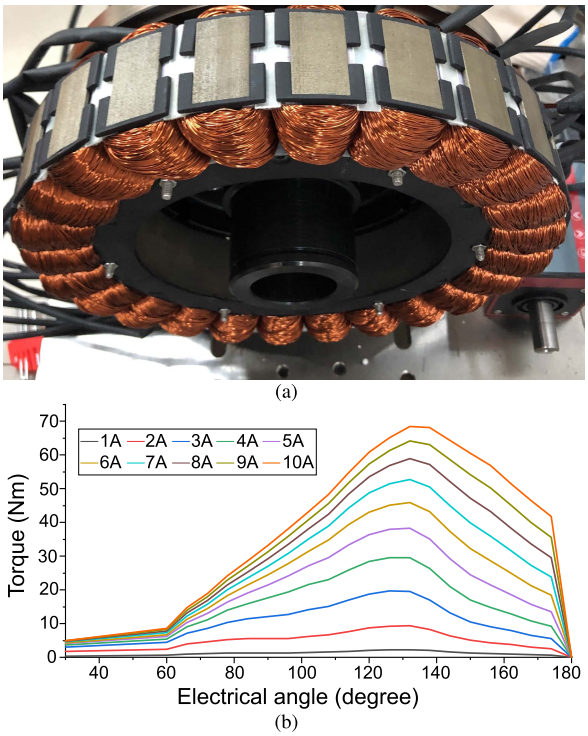

FIGURE 1. Prototype and output characteristic of 24/16 direct-drive SRM. (a)Prototype of designed DDSRM. (b)Torque versus current and rotor position for designed DDSRM.

TABLE 1. Structure parameters of direct-drive 24/16 out-rotor DDSRM designed for washing machine.

Parameters	Values
Number of stator poles	24
Number of rotor poles	16
Rotor outer diameter (mm)	294
Rotor inner diameter (mm)	250
Stator outer diameter (mm)	249.4
Stator inner diameter (mm)	140
Stack length (mm)	35
Stator arc angle (deg)	10.3
Rotor arc angle (deg)	8
Winding turns	48

multi-objective optimization [22]. The structure of DDSRM is shown in Fig. 1 (a), the torque - current - position curve of DDSRM are given in Fig. 1 (b). Structure parameters of DDSRM are illustrated in Tab. 1. It can be see from Fig. 1 (b) that output torque of DDSRM can reach 35 N·m at 10 A, DDSRM can satisfy output torque requirement within current limitation. However, phase inductance of DDSRM are high, maximum speed of DDSRM is limited due to high back-EMF, VSPW of the proposed SRM need to be increased to broaden speed range.

B. SRM DRIVE TOPOLOGY

VSPW of DDSRM is decided by drive topology and winding topology. Conventional SRM drive system is consisted of power converter, driver module for power switches, controller and sensors (such as encoder and current transducers). Asymmetric half-bridge power converter is widely used for SRM considering its fault tolerance capability, in which each phase is independently controlled by power switches. A 3-phase

SRM drive system with asymmetric half-bridge power converter is shown in Fig. 2. For proposed DDSRM, each phase is consisted of 8 winding coils, winding coils from different phase are arranged regularly.

Coils belong to one phase connect with each other in certain topology and finally form a dual-port winding, port voltage (the port connected with positive pole of power supply is defined as positive port) of each winding are regulated by two power switches in asymmetric half-bridge power converter, the actions of two power switches leads to different port voltage:

1) Positive port voltage: when two switches are both conducting, the port voltage equals to bus voltage. With positive port voltage, winding current increases.
2) Zero port voltage: when one power switch is turned off and another keep conducting, the port voltage equals to zero, winding current decreases slowly with cooper loss.
3) Negative port voltage: when two switches are both turned off, winding storage energy is feeded back to power supply, the port voltage equals to negative bus voltage until tail current decreases to zero.

VSPW is the voltage that implemented on coils of single pole, the relationship between VSPW and winding voltage depends on winding topology of SRM.

C. WINDING TOPOLOGY OF SRM

Winding topology refers to connection method between coils belong to same winding. The coils distribution for 3-phase 24/16 SRM is illustrated in Fig. 3 (a), all possible connection topologies for phase A are illustrated in Fig. 3 (b)-(d), namely serial topology, hybrid topology and parallel topology, respectively. The port voltage for each winding equals to bus voltage when corresponding power switches are conducting, however, VSPW is different depends on winding topology.

Without considering manufacutring error and structure imbalance, the resistance of each coil should be equal, so as VSPW (U_{wd}) and coil current (i_{wd}):

$$i_{wd} = i_k(k = 1, 2..8) \tag{1}$$

$$U_{wd} = U_k(k = 1, 2..8) \tag{2}$$

The relationship between port voltage and VSPW, and the relationship between bus current and coil current, both depends on the winding topology.

For serial topology:

$$i_{bus} = i_{wd} \tag{3}$$

$$U_{bus} = 8 * U_{wd} \tag{4}$$

For hybrid topology:

$$i_{bus} = 2 * i_{wd} \tag{5}$$

$$U_{bus} = 4 * U_{wd} \tag{6}$$

For parallel topology:

$$i_{bus} = 4 * i_{wd} \tag{7}$$

$$U_{bus} = 2 * U_{wd} \tag{8}$$

where i_{bus} and U_{bus} represent port current and port voltage of one phase, respectively. According to voltage equation of winding coil:

$$U_{wd} = \frac{d\phi_{wd}}{dt} + i_{wd} * R_{wd} \tag{9}$$

where ϕ_{wd} and R_{wd} are flux linkage and resistance of one coil. It can be conclude that dynamic variation of flux linkage and current depends on coil voltage, thus, different current waveforms exist with same control parameters in different topologies, Fig. 4 gives phase current of SRM with three topologies that operating under single-pulse mode with same speed and load. The difference between current waveforms lies in the rate of current rise and fall. With serial topology, VSPW is minimum and winding current rises gently for SRM, the corresponding winding needs to be switched on in advance to prolong the dwell period and guartee torque capability. The switching angle moves rearward as VSPW increase, thus, current waveforms for SRM with hybrid and parallel topology are different. As current waveform correlates with many performance criterias, it can be conjectured that winding topoloy has significatn influence on SRM performance.

D. EFFECT OF WINDING TOPOLOGY ON SRM PERFORMANCE

The effect of winding topology on SRM performance is studied through numerical method. A multi-physics simulation method is implemented using ANSYS Workbench, the diagram for multi-physics simulation is given in Fig. 5. Dual-coupling between electromagnetic force calculation and mechanical load is built, electromagnetic field distribution and electromagnetic force (Te) of DDSRM with different winding voltage (U_{wd}) are dynamically calculated using FEM in Maxwell, rotor velocity (ω) and position (θ) are calculated through coupling electromagnetic force with mechanical load and then feedback to SRM controller. The winding voltages of DDSRM are regulated by drive circuit and winding topology control module which are implemented in Simplorer. Control signals for drive circuit (S_{dr}) are generated by switching angle control according to electromagnetic characteristic of DDSRM and feedback of velocity, position and current. Control signals for winding topology (S_{tp}) are generated by winding topology control according to velocity, both switching angle control and winding topology control are built in Matlab.

The performance of 3-phase 24/16 DDSRM with different winding topology is acquired through high fidelity multi-physics simulation. The power source for DDSRM drive is AC 220V, the bus voltage of DDSRM drive is acquired through AC-DC rectifier. DDSRM works on single-pulse control mode in simulation, turn-on and turn-off angle are selected using optimal switching angle control method proposed in Section IV. The efficiency of DDSRM are compared with different speed and mechanical load,

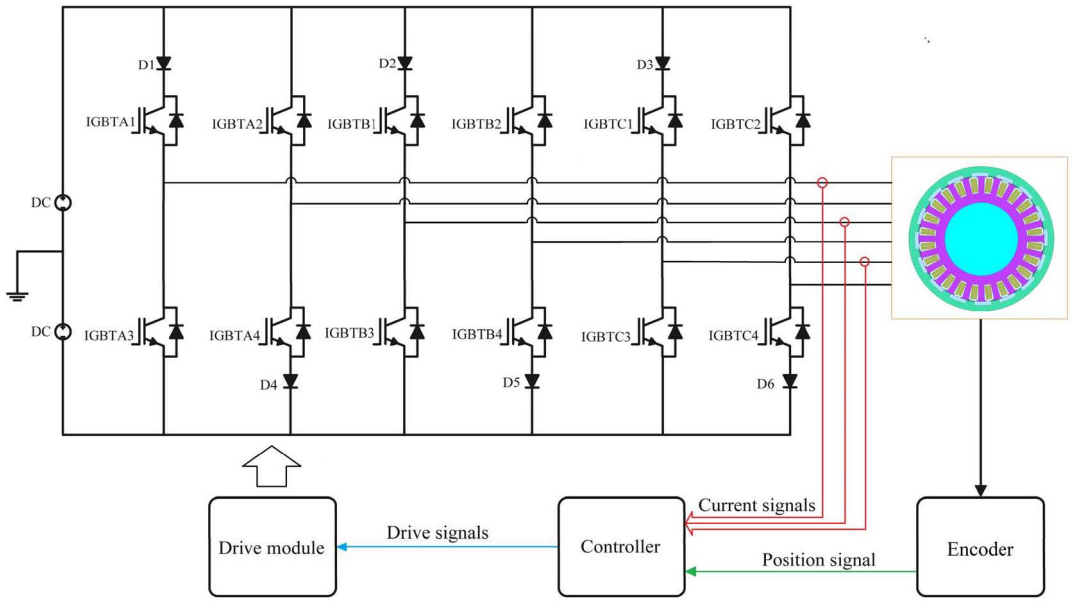

FIGURE 2. Drive system for 3-phase SRM.

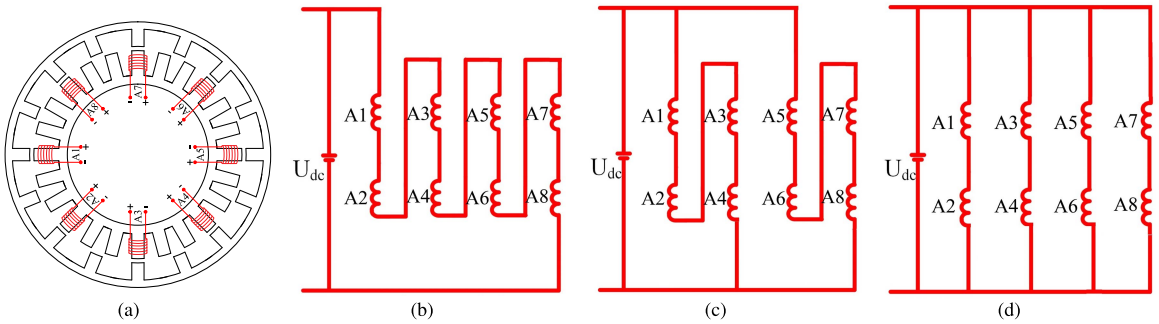

FIGURE 3. Winding topologies for 3-phase 24/16 DDSRM. (a) Coils distribution for DDSRM. (b) Serial topology. (c) Hybrid topology. (d) Parallel topology.

the efficiency-speed characteristic with mechanical loads of 3N·m, 10N·m, 18N·m, and 25N·m are given in Fig. 6(a)-(d). respectively. The speed with maximum efficiency for each winding topology are marked, the speed when motor efficiency for two different winding topologies are identical are also marked.

Fig. 6(a) shows that motor efficiency with serial winding is better than other winding topology with speed under 618 rpm. For DDSRM with serial winding topology and 3 N·m mechanical load, motor efficiency increases as speed increase until speed reaches 560 rpm; when speed exceeds 560 rpm, motor efficiency decreases as speed increase, the maximum efficiency is 89%. Motor efficiency for DDSRM with serial winding topology and hybrid winding topology are the same at speed of 618 rpm, motor efficiency with hybrid winding will be better than other winding topology between 618 rpm and 1235 rpm, the maximum efficiency for DDSRM with hybrid winding exists at 953 rpm with value 92%. Motor efficiency of DDSRM with hybrid topology decrease as speed exceeds 953 rpm. Motor efficiency for DDSRM with hybrid winding topology and parallel winding topology are the same at 1235 rpm. Motor efficiency for DDSRM with parallel winding topology will be better than other case when speed exceeds 1235 rpm, the maximum efficiency for DDSRM with parallel winding topology exists at 1562 rpm with value 91%. We can see from Fig. 6(b), Fig. 6(c) and Fig. 6(d) that under different load, motor efficiency for DDSRM with different winding topology show similar relationship, motor efficiency tends to increase as speed increase until a turning point, then motor efficiency decrease as speed increase, maximum efficiency exists on different speed with different topology.

Maximum bus current for DDSRM with different winding topology under different speed and load are shown in Fig. 7. For same working condition, DDSRM with parallel topology has biggest bus current, while DDSRM with serial topology has minimum bus current. For all types of winding topologies, maximum bus current decrease as speed increase due to adjustment in switching angles. Notably, the difference in maximum bus current is significant between different topology, however, the conduction angle decrease as VSPW increase, the conduction angle for parallel topology will be smaller than other topologies, the difference in output power will be smaller than that in maximum bus current.

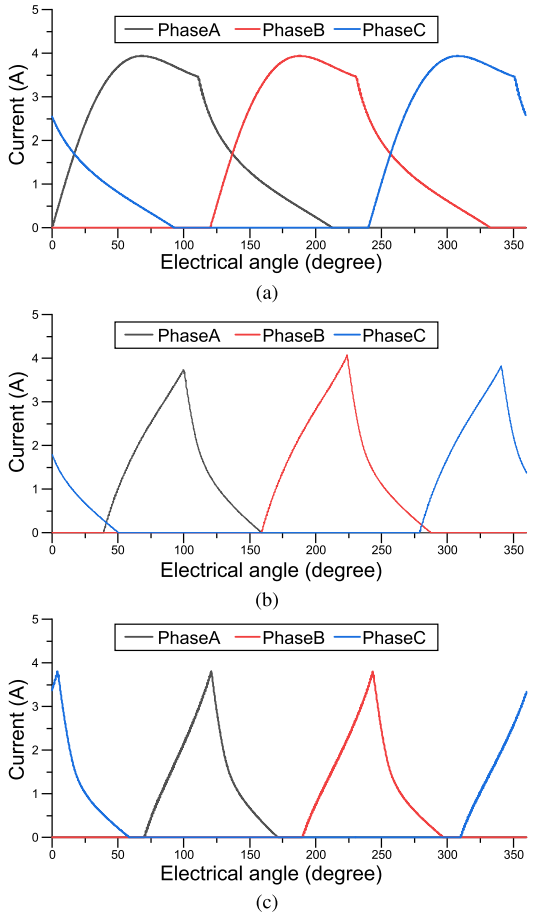

FIGURE 4. Current waveforms of DDSRM with three topologies. (a)Serial. (b)Hybrid. (c)Parallel.

From Fig. 6 and Fig. 7, we can see DDSRM with serial topology are suitable to operate at low speed when back-EMF is low, DDSRM with other topology could also operate at low speed, however, the bus current would be higher than DDSRM with serial topology, which introduce more copper loss. As speed increase, DDSRM with hybrid topology would has better efficiency, meanwhile, maximum bus current also decrease. DDSRM with parallel topology are suitable to operate at high speed, DDSRM with other topology could not reach high speed due to low VSPW. There are interaction points where two types of winding topology have same efficiency, it is reasonable to switch winding topologies at intersection points considering motor efficiency. These interaction points are listed in Tab. 2. With the interaction points given in Tab. 2 as segmentation points, we approximate the relation between interaction speed and load with a piecewise linear curve, which could be used to determine optimal switching speed for other load.

III. IMPLEMENTATION AND CONTROL STRATEGY FOR RECONFIGURABLE TOPOLOGY SRM

According to effect of winding topology on DDSRM performance, switching winding topology according to speed and load may leads to better performance. In this section, a new DDSRM driver system with capability to switch topologies adaptively will be proposed, the hardware of driver system and corresponding control strategy to switch topology are illustrated.

TABLE 2. Interaction points between different topology for 24/16 out-rotor DDSRM considering efficiency.

Mechanical load (N·m)	Optimal switching point 1 (serial->hybrid)	Optimal switching point 2 (hybrid->parallel)
3	618	1235
10	575	1036
18	341	803
25	296	602

A. HARDWARE IMPLEMENTATION TO SWITCH TOPOLOGY

The reconfigurable topology in this paper does not change the structure of power converter, but change the connection of winding coils via topology switching module. Topology switching module is consist of relays and change connection state through energizing/de-energizing relay coil.

In this paper, a 24/16 3-phase DDSRM is used. Take phase A as example, there are eight pole windings for phase A, pole winding coils connect each other through relays, which is different from conventional fixed connection. The relays are used to change winding topology conveniently, each relay has three contacts, named intermediate contact (IC), normally closed contact (NCC) and normally open contact (NOC), respectively. IC is connecting with NCC if relay coil is de-energized, meanwhile NOC remains unconnected; when relay coil is energized, IC would connect with NOC instead, NCC will be disconnected. Six relays are used to swtich between three topologies, the connection between relays and pole winding coils are shown in Fig. 8. By adjusting the status of the relay coil, three different types of winding topology can be obtained.

1) Parallel topology: relay K2, K4 and K6 are powered on, IC in such relays switched to NOC,, while IC in other relays connects to NCC.
2) Hybrid topology: relay K1, K4 and K5 are powered on, IC in such relays switched to NOC, while IC in other relays connects to NCC.
3) Serial topology: relay K1, K3 and K5 are powered on, IC in such relays switched to NOC; while IC in other relays connects to NCC.

The status of relay are regulated by DDSRM controller, realy coil, output buffer circuit and external power supply are connected. Relay coil would be powered by external power supply when output buffer is switched on, and IC will switched to NOC once corresponding coil is powered, otherwise IC will connects with NCC. The topology of DDSRM winding could be changed according to control signal of the controller.

B. TOPOLOGY SWITCHING STRATEGY

According to the influence of winding topology on DDSRM performance, each winding topology has optimum velocity range within which its efficiency is better than other

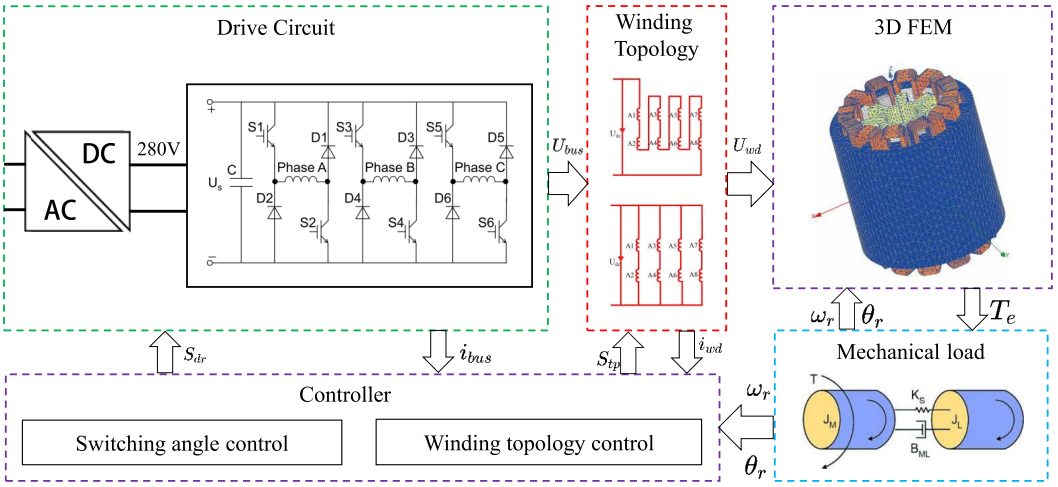

FIGURE 5. Diagram for multi-physics simulation.

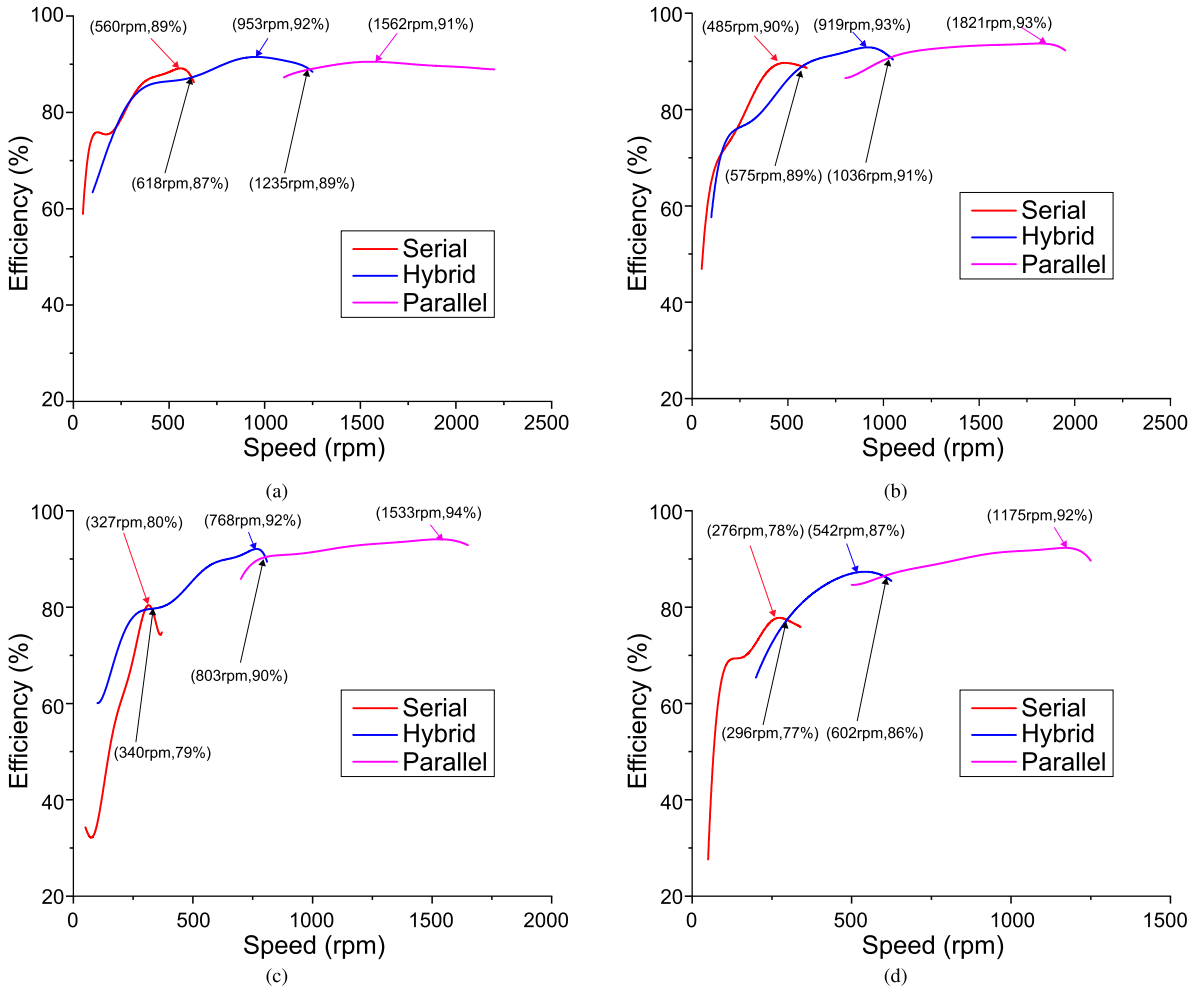

FIGURE 6. Efficiency of DDSRM different topologies and mechanical load. (a)3 N·m. (b)10 N·m. (c)18 N·m. (d)25 N·m.

topologies. Switching winding topology according to velocity could lead to better overall performance. We name speed that two types of winding topology has same efficiency as critical speed, there are two critical speed between three types of winding topology, DDSRM with serial winding topology and hybrid winding topology have same performance at first critical speed, while DDSRM with hybrid winding topology and parallel winding topology have same performance at second critical speed. The flowchart to switch winding topology is shown in Fig.9, velocity of DDSRM is monitored, a winding topology selection strategy will be conducted according to velocity. When velocity is lower than first critical speed,

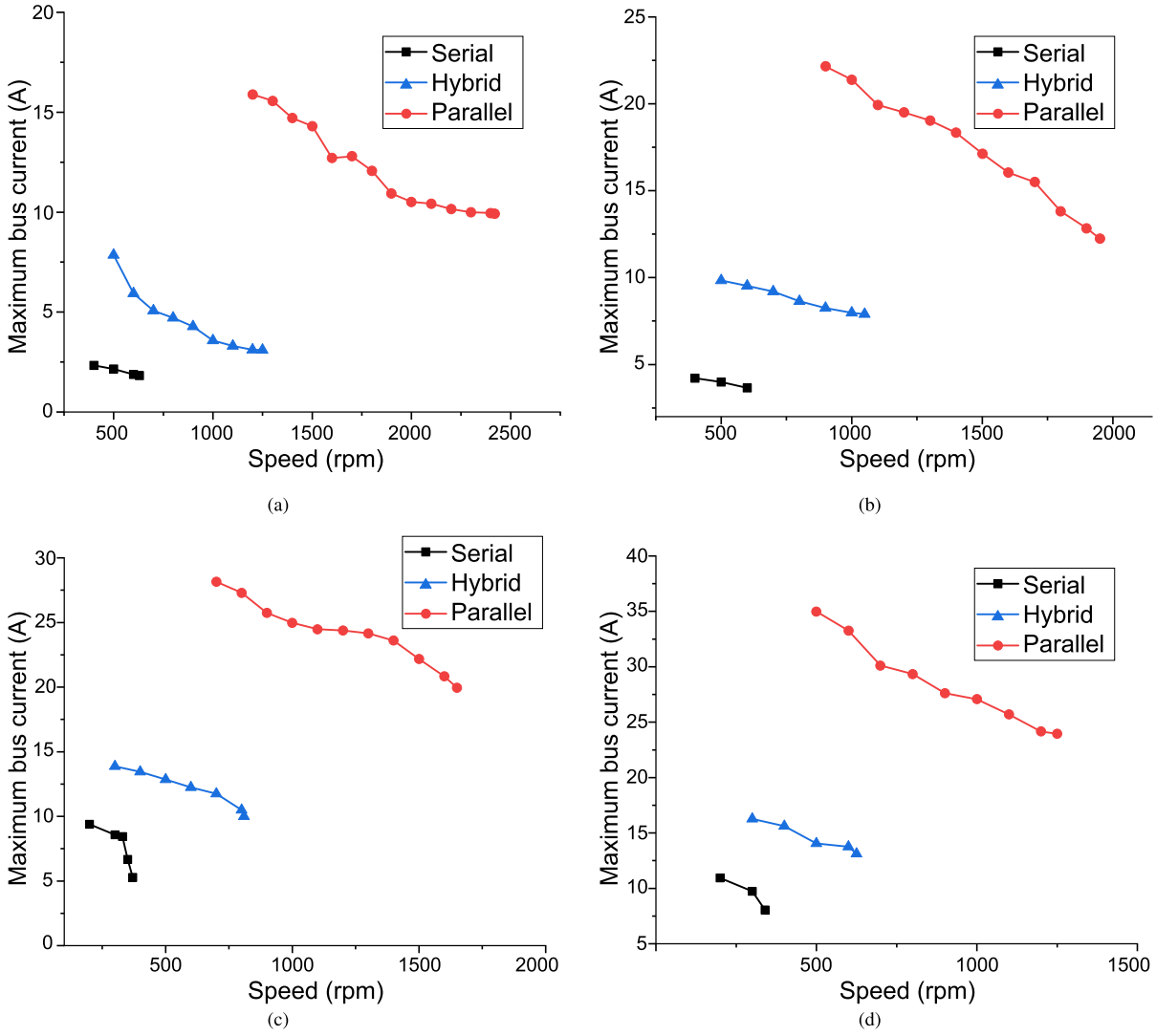

FIGURE 7. Maximum bus current with different load. (a)3 N·m. (b)10 N·m. (c)18 N·m. (d)25 N·m.

DDSRM will switch to serial topology, relay K1, K3 and K5 will be energized; when velocity is between first critical speed and second critical speed, DDSRM will switch to hybrid topology, relay K1, K4 and K5 will be energized; when velocity is greater than second critical speed, DDSRM will switch to parallel topology, relay K2, K4 and K6 will be energized. Notable, to avoid transient oscillation of phase current, the winding topology switching would be implemented only when one phase is turned off.

IV. OPTIMAL TURN-ON AND TURN-OFF ANGLE SELECTION

Turn-on and turn-off angles are important parameters that affect SRM efficiency. In this paper, single-pulse control (SPC) strategy is used. To ensure DDSRM have maximum efficiency in each operating condition, the turn-on and turn-off angles need to be adjusted, the selection method will be discussed in this chapter.

The relationship between switching angles and power loss of DDSRM is first investigated, a fast power loss calculation model is built. Without considering stray loss, power loss of SRM includes copper loss and iron loss. Copper loss of SRM is proportional to square of phase current, however, calculation of iron loss for SRM is relatively complicated due to double salient pole structure of SRM and non-sinusoidal current waveform.

With SPC, flux linkage increase linearly after turn-on angle, as shown in Fig.10. Flux linkage, as well as current waveform, depend on switching angles and velocity. Linear flux linkage model (LFLM) will be used to calculate optimal turn-on and turn-off angles.

$$\phi(\theta) = \begin{cases} \frac{U}{\omega}(\theta - \theta_{on}) & \theta_{on} < \theta < \theta_{off} \\ \frac{U}{\omega}(2\theta_{off} - \theta_{on} - \theta) & \theta_{off} < \theta < 2\theta_{off} - \theta_{on} \\ 0 & other \end{cases} \tag{10}$$

As shown in Fig.11, the magnetic field density is different at different position of DDSRM. To calculated iron loss concisely, flux path of DDSRM is separated into four regions

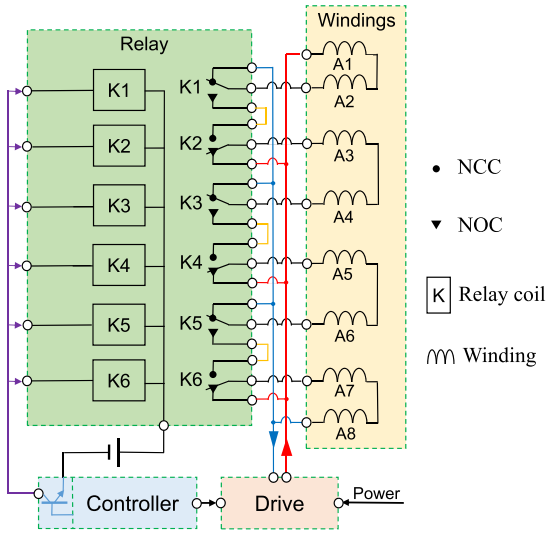

FIGURE 8. Hardware implementation to switch winding topology.

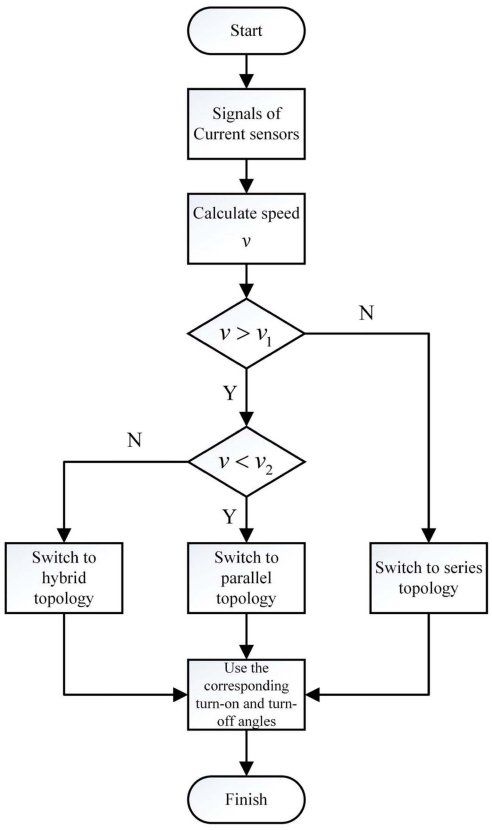

FIGURE 9. Flow chart for topology switching strategy.

(stator teeth, stator yoke, rotor teeth and rotor yoke), magnetic field density distributes relative uniformly in each region, iron loss of each region can be calculated according to magnetic field density and regional volume. The steps to build fast power loss calculation model and optimize turn-on and turn-off angle are as follows:

1) Use LFLM to calculate flux linkage within one electrical period under different turn-on and turn-off angle. Calculate flux density at different regions of DDSRM with respect to rotor position, including stator teeth, stator yoke, rotor teeth and rotor yoke.
2) Calculate copper loss of DDSRM. Magnetic resistance (1/L) is presented as Fourier series, current harmonics can be obtained using ϕ/L, total copper loss of DDSRM can be calculated by superposition of copper loss caused by current harmonics.
3) Calculate iron loss of DDSRM. Flux density at each region is decomposed to obtain its harmonics, calculate iron loss of each region based on Steinmetz formula. Total iron loss of DDSRM equals to superposition of iron loss of all regions.
4) Power loss of DDSRM consists of iron loss and copper loss. Build relationship between DDSRM efficiency, velocity and switching angles according to fast power loss calculation model.
5) Find optimal switching angles through iterative searching method.

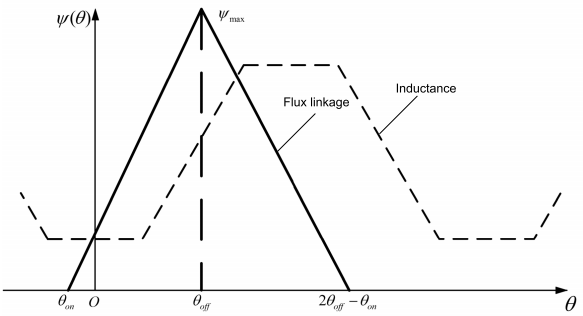

FIGURE 10. Flux linkage versus rotor position under SPC mode.

The distribution of flux linkage at different regions of DDSRM depends on rotor position. Flux linkage for each phase winding are represented as ϕ_A, ϕ_B, and ϕ_C, and the number of turns for each phase winding is N_p. The positive direction for stator/rotor teeth flux is from inner diameter to outer diameter, and positive direction for stator/rotor yoke flux is clockwise. The magnetic flux in different part of DDSRM can be acquired according to magnetic circuit theory [23].

Stator teeth flux ϕ_{sp} can be represented as (11):

$$\begin{aligned}\phi_{spA}(\theta) &= \frac{\phi_A(\theta)}{N_p} \\ \phi_{spB}(\theta) &= \frac{\phi_B(\theta)}{N_p} = \phi_A(\theta + \frac{2}{3}\pi) \\ \phi_{spC}(\theta) &= \frac{\phi_C(\theta)}{N_p} = \phi_A(\theta + \frac{4}{3}\pi)\end{aligned} \tag{11}$$

The stator yoke flux ϕ_{sc} can be represented as 12:

$$\begin{aligned}\phi_{sc1}(\theta) &= \frac{1}{2}(\phi_{spA}(\theta) + \phi_{spB}(\theta) + \phi_{spC}(\theta)) \\ \phi_{sc2}(\theta) &= \frac{1}{2}(\phi_{spA}(\theta) + \phi_{spB}(\theta) - \phi_{spC}(\theta)) \\ \phi_{sc3}(\theta) &= \frac{1}{2}(\phi_{spA}(\theta) - \phi_{spB}(\theta) - \phi_{spC}(\theta))\end{aligned} \tag{12}$$

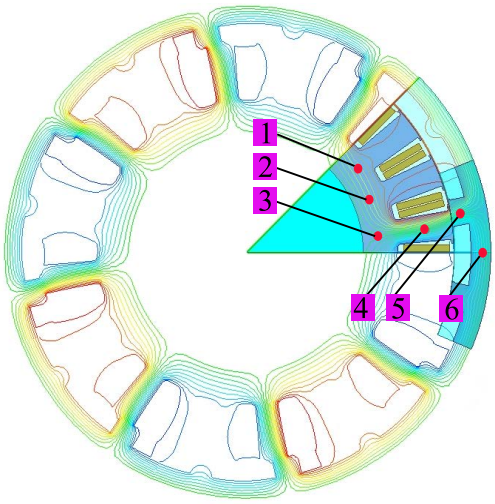

FIGURE 11. The selected points along magnetic circuit for comparison between analytical model and FEM.

The rotor teeth flux ϕ_{rp} can be represented as 13:

$$\begin{aligned}\phi_{rp1}(\theta) &= \frac{1}{2}(\phi_{spA}(\theta)\\ \phi_{rp2}(\theta) &= \frac{1}{2}(\phi_{rp1}(\theta + 2\pi)\end{aligned} \tag{13}$$

The rotor yoke flux ϕ_{rc} can be represented as 14:

$$\begin{aligned}\phi_{rc1}(\theta) &= \frac{1}{2}(\phi_{spA}(\theta) - \phi_{spB}(\theta) - \phi_{spC}(\theta))\\ \phi_{rc2}(\theta) &= \phi_{rc1}(\theta + 2\pi)\\ \phi_{rc3}(\theta) &= \phi_{rc1}(\theta + 4\pi)\end{aligned} \tag{14}$$

Based on the above equations, flux linkage at each region of DDSRM can be calculated. To verify the accuracy of magnetic field density at different region, six points are selected to record magnetic field density of DDSRM with load of 3 N.m at 500 rpm through FEM, and will further compared with the proposed equations. As shown in Fig. 11, the selected points locate at stator yoke, stator teetch, rotor teetch, and rotor yoke. The comparison results of magnetic field density at selected points are shown in Fig. 12.

It can be seen from Fig. 12 that equations (11 - 14) are effectively in predicting magnetic field density of DDSRM in different regions. Notable, Fig. 12 only gives magnetic field density at different region for unsaturated condition, however, the relation between flux linkage and magnetic field density along magnetic circuit is not affected by magnetic saturation, equations (11-14) are also applicable for saturated condition. With such analytical model, the harmonics of magnetic field density in each region of DDSRM can be obtained through Fourier transformation. The iron loss of each region can be calculated using Steinmetz formula as 15.

$$P_{fe} = C_h f \sum_{k=1}^{m} k B_m^n + C_e f^2 \sum_{k=1}^{m} k^2 B_m^2 \tag{15}$$

where C_h and C_e represent hysteresis loss coefficient and eddy current loss coefficient of iron core, respectively. They can be obtained from silicon steel manufacturer.

Once fast power loss calculation model is built, the relationship between motor efficiency and control parameters (turn-on and turn-off angle) can be developed, and optimal switching angles that increase motor efficiency can be obtained by genetic algorithm. Fig.13 shows optimal turn-on and turn-off angles obtained based on fast power loss calculation model.

V. EVALUATION OF DDSRM PERFORMANCE WITH RECONFIGURABLE WINDING TOPOLOGY

A. SIMULATION

The performance of DDSRM with topology switching control and optimal switching angle control are evaluated using multi-physics simulation. The topology switching point and optimal turn-on and turn-off angles in simulation are given in Tab.2 and Fig. 13.

Torque-speed characteristic of DDSRM with different topology are given in Fig.14. For low speed and high torque condition, serial topology will be used. It can be seen from Fig.14(a) that maximum torque can reach 61 N·m at 50 rpm, which accommodates the requirement of maximum torque for DDSRM using in rinse mode, however, the maximum speed with serial topology is limited by 670 rpm with load of 3 N·m. For high speed, parallel topology will be used, it can be seen from Fig.14(b) that maximum speed can reach 2100 rpm with load of 3 N·m. The requirement of high operating speed in dehydration mode is satisfied. It can be deduced from Fig.14 that DDSRM with onefold topology can't satisfy the requirement to work at low speed with high torque while maintain wild speed range, the topology switching strategy is crucial for DDSRM to use in washing machine.

The efficiency of DDSRM with reconfigurable winding topology is given in Fig. 15. DDSRM can achieve speed range of 50 rpm - 2200 rpm with load of 3 N·m, motor efficiency is above 60% within speed range. With load of 25 N·m, DDSRM can reach up to 1120 rpm. Motor efficiency for DDSRM operating at 50 rpm with load of 25 N·m is relatively low, phase current is high to generate required torque, cooper loss dominates power consumption in this condition, which leads poor performance of DDSRM. Motor efficiency increase rapidly as velocity increase with load of 25 N·m, it could reach 64% when velocity exceeds 70 rpm. The simulation results convince that topology switching strategy and optimal switching angle control work well, the proposed DDSRM with reconfigurable winding topology can meet performance requirements of washing machines.

B. EXPERIMENT

The performance of DDSRM is evaluated in experiments. The experimental setup is shown in Fig.16, a 24/16 3-phase DDSRM is fabricated and used in experiment, structure of the prototype are consistent with that used in simulation. A magnetic powder brake is used as mechanical load, torque transducer is assembled between DDSRM and magnetic powder brake to measure output torque as shown in

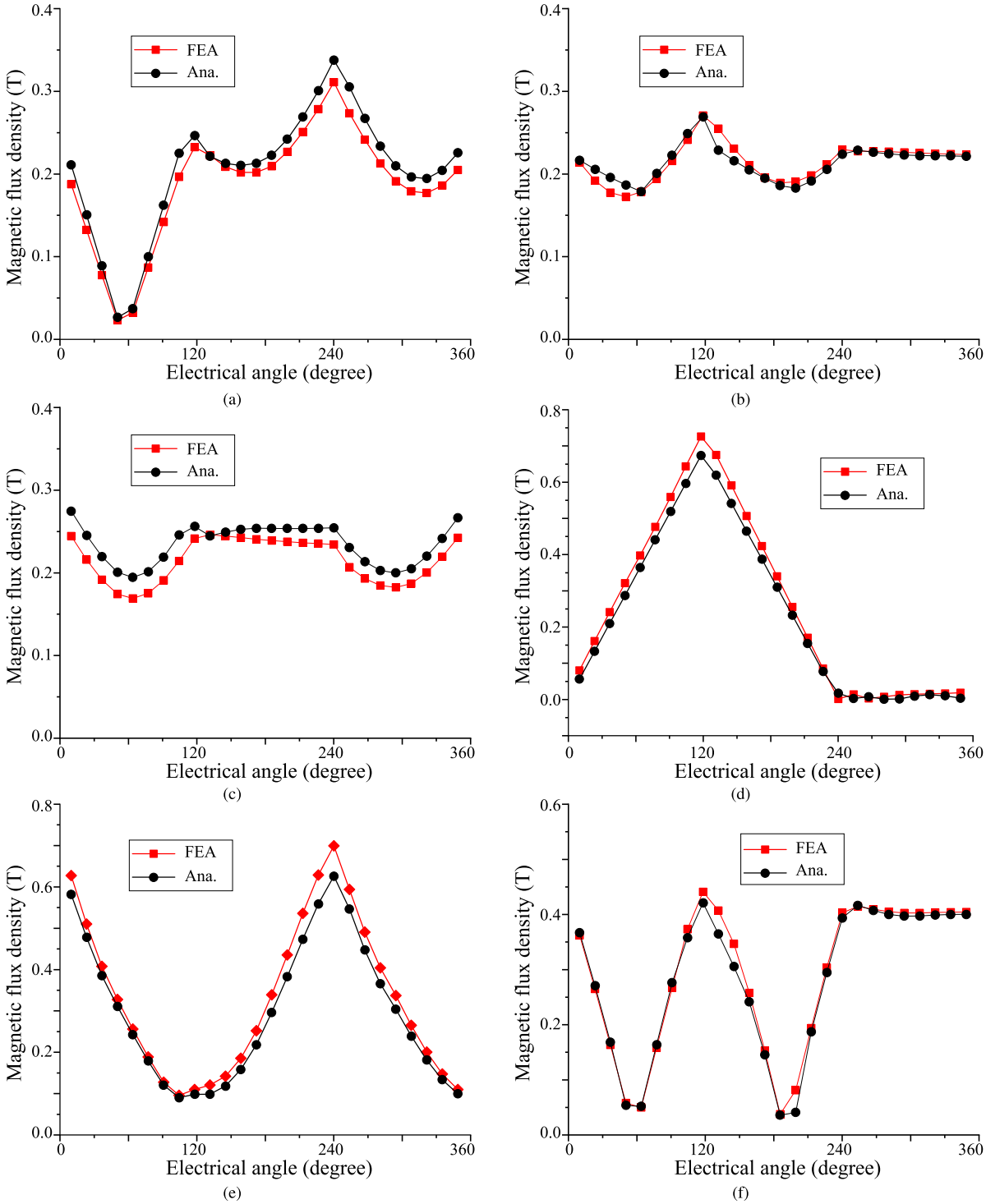

FIGURE 12. Comparison of magnetic field density in different regions of DDSRM between FEM and analytical method. (a)Point 1. (b)Point 2; (c)Point 3; (d)Point 4; (e)Point 5; (f)Point 6.

Fig. 16(a). Pole windings of the prototype are connected through relays as shown in Fig. 16(b), winding topology is switched when relay state change. DDSRM driver is shown in Fig. 16(c); SPC is used to regulate DDSRM speed, the control program is implemented on DSP TMS320F2812 as shown in Fig. 16(d). Both phase current, output torque and velocity are sample through data acquisition (DAQ) card to calculate motor efficiency. The control system for DDSRM is given in Figure 16. Considering load uncertain in experiment and real application, an online turn on/off angle adaption mechanism is embedded into the speed control loop. A PI controller is used to generate torque command according to speed error between real speed and speed command. The torque command, as well as two look-up tables (LUTs), are

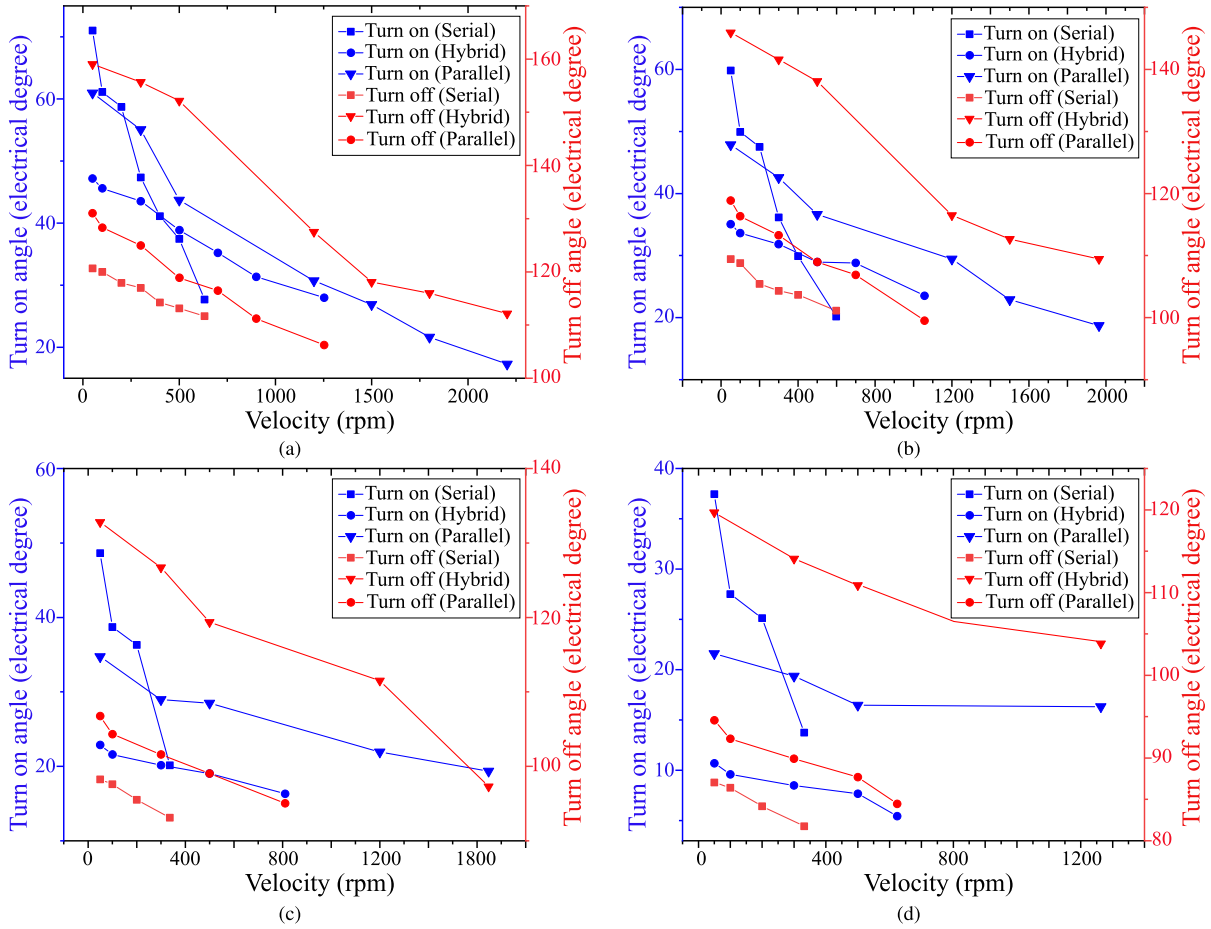

FIGURE 13. Optimum switching angles for DDSRM with different winding topology. (a) 3N·m. (b)10N·m. (c)18N·m. (d)24N·m.

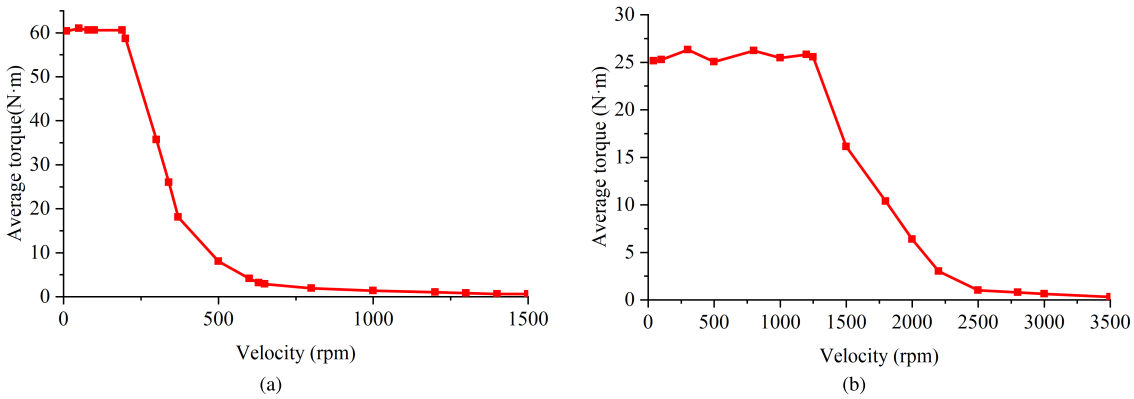

FIGURE 14. Torque-speed characteristic of DDSRM with different topology. (a) Serial topology. (b)Hybrid topology.

used to determine winding topology and optimal switching angles. LUT 1 is a 1D interpolation table between interaction speed and torque. Topology control module calculate interaction speed according to torque command from LUT 1, and then determine which winding topology to be implemented through comparing interaction speed and current speed. LUT 2 is a 2D interpolation table between switching angles, speed and torque, which is generated according to optimal switching angles given in Figure 13. Switching angle control module calculate optimal switching angles according to torque command and current speed from LUT 2. Optimal switching angles are then used to generated drive signals for power converter. The parameters P and I are tuned according to DDSRM performance in experiment.

Before measuring efficiency, the stray losses, caused by friction, wind resistance and shaft eccentricity, need to be calibrated. DDSRM operated at different velocity with brake unpowered, phase current are recorded and used to calculate power input without mechanical load (PIOML), PIOML should be considered to accurately calculate efficiency

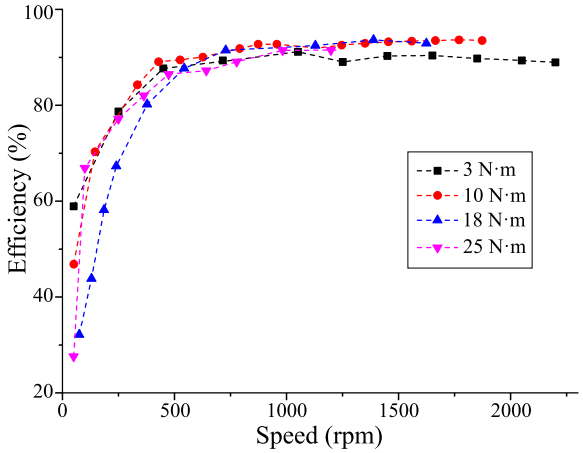

FIGURE 15. Efficiency of DDSRM with different velocity and mechanical load.

of DDSRM. When calculating DDSRM efficiency, output power of DDSRM are calculated by combine PIOML and brake load.

The experimental tests are conducted under load of 3N·m, 10N·m, 18N·m, and 25N·m, respectively. Both topology switching strategy and optimal switching angle control are implemented. Phase current and bus current are recorded between 50 rpm -1500 rpm according to requirement of washing machine. When velocity reaches topology switching point, DDSRM can automatically switch the winding topology. Fig.18 shows phase currents of DDSRM with different winding topology under load of 3N·m at 100 rpm, we can see current waveforms of DDSRM with three winding topologies are different.

Both input power and ouput power of DDSRM are calculated based on DAQ datas, then DDSRM efficiency can be calculated. The efficiency-velocity map can be obtained with different load, as shown in Fig.19. Maximum velocity of DDSRM can reach 1520 rpm with load of 3 N·m, while it can also reach 810 rpm with load of 25 N·m. The proposed DDSRM with reconfigurable winding topology can meet performance requirements of washing machines.

With load of 3 N·m, serial topology is adopted when velocity is under 620 rpm, motor efficiency of DDSRM is 46% at 50 rpm and keep increasing as velocity increase. However, motor efficiency for DDSRM with serial topology achieve its maximum value at 600 rpm, motor efficiency at 620 rpm is lower than that of 600 rpm, then, winding topology is switched to hybrid topology at 620 rpm, motor

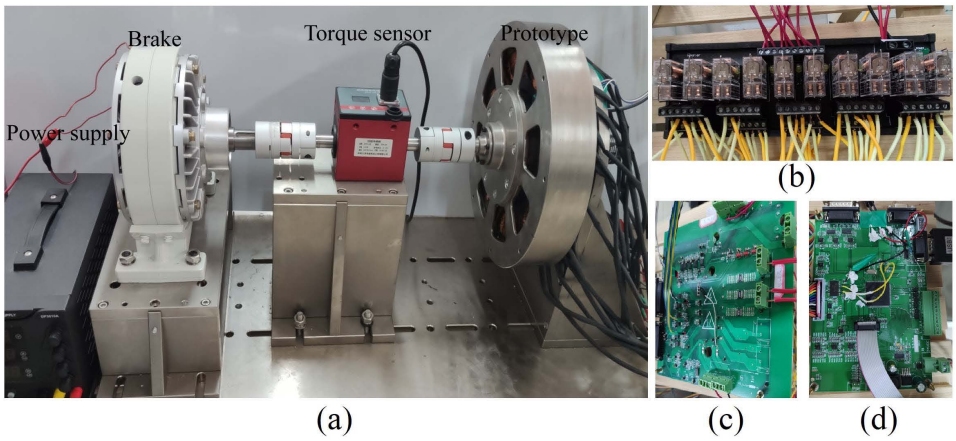

FIGURE 16. Experimental setup for DDSRM with reconfigurable winding topology. (a)Loading device, (b)Topology switching module, (c)Motor drive, (d)Control module.

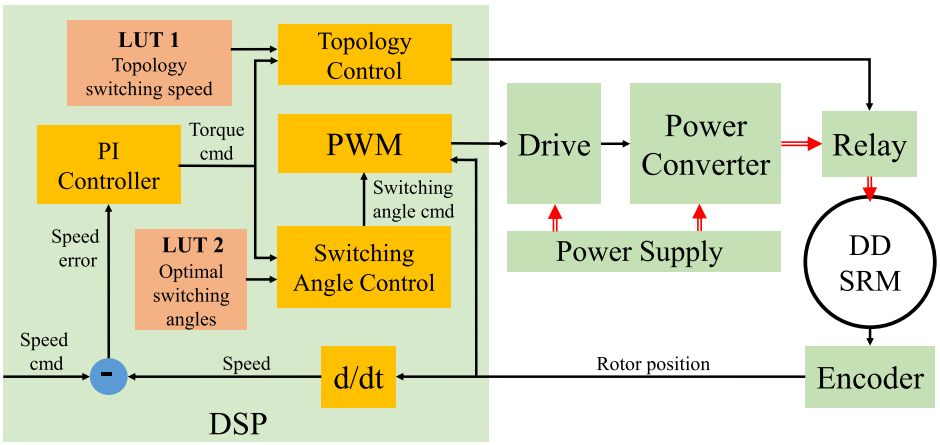

FIGURE 17. Scheme of control system for DDSRM.

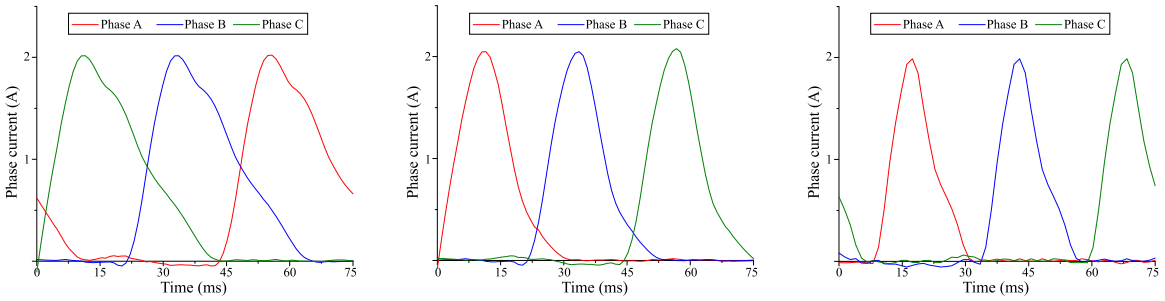

FIGURE 18. Current waveforms of DDSRM with different topology in experiment. (a) Serial topology. (b)Hybrid topology. (c)Parallel topology.

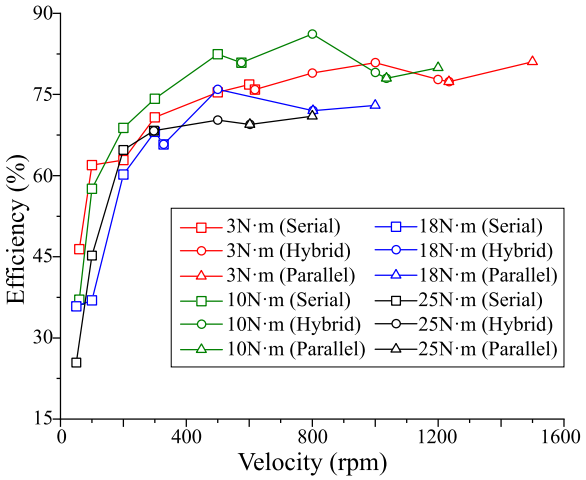

FIGURE 19. DDSRM efficiency with different velocity and mechanical load in experiment.

efficiency keep increasing after switching to hybrid topology. Efficiency of DDSRM with hybrid winding topology reaches its maximum value at 980 rpm, then winding topology is switched to parallel type at 1050 rpm. After winding topology switching to parallel type, motor efficiency of DDSRM begins to increase. With load of 10 N·m, 18 N·m and 25 N·m, efficiency of DDSRM with three topologies show similar relationship. The experiments demonstrate that efficiency of DDSRM is improved by switching winding topology.

Comparing Fig. 15 and Fig. 19, it is found that DDSRM efficiency obtained from experiment is slightly lower than that obtained from simulation, iron loss calculated by FEM is lower than actual value due to neglection of saturation effect and flux leakage. Notable, although we have taken PIOML into account when calculating efficiency, there are other factors that lead to difference in efficiency between simulation and experiment, such as manufacture and assemble errors of porotype, nonlinearity of frictional losses. When the total power consumption become small, the influence of such factors would be more significant. For example, the experimental efficiency at 100 rpm and 3 N·m is 47%, while simulation shows an efficiency above 60%.

VI. CONCLUSION

In this paper, a new type of direct-drive motor system is proposed for washing machines, which requires high torque output at low speed while maintaining wild speed range. The concept of reconfigurable winding topology is proposed to expand operation range of DDSRM.The effect of winding topology on DDSRM efficiency is analyzed through multi-physics simulation, then topology switching strategy for DDSRM are determined. Since turn-on and turn-off angles have significant effect on motor efficiency, the relationship between motor efficiency and switching angles is deduced theoretically, optimal turn-on and turn-off angles for DDSRM with different topologies under different operating conditions are given. Both simulation and experiments are conducted to evaluate performance of DDSRM with reconfigurable winding topology, the results demonstrate that topology switching strategy and optimal switching angels control could improve DDSRM efficiency. DDSRM with reconfigurable winding topology is of great value in promoting direct-drive technology for washing machines and facilities with similar operating condition, such as hydraulic system and aerospace actuators.

REFERENCES

[1] R. Stamminger, A. Bues, F. Alfieri, and M. Cordella, "Durability of washing machines under real life conditions: Definition and application of a testing procedure," *J. Cleaner Prod.*, vol. 261, Jul. 2020, Art. no. 121222.

[2] C.-S. Jin, D.-S. Jung, K.-C. Kim, Y.-D. Chun, H.-W. Lee, and J. Lee, "A study on improvement magnetic torque characteristics of IPMSM for direct drive washing machine," *IEEE Trans. Magn.*, vol. 45, no. 6, pp. 2811–2814, Jun. 2009.

[3] W. Cheng, H. Zhiwei, and G. Jinian, "The application of a novel motor in washing machines," in *Proc. 5th Int. Conf. Electr. Mach. Syst. (ICEMS)*, vol. 2, Aug. 2001, pp. 1030–1033.

[4] S. M. Castano, R. Yang, C. Mak, B. Bilgin, and A. Emadi, "External-rotor switched reluctance motor for direct-drive home appliances," in *Proc. 44th Annu. Conf. IEEE Ind. Electron. Soc. (IECON)*, Oct. 2018, pp. 514–521.

[5] M. Asgar, E. Afjei, A. Behbahani, and A. Siadatan, "A 12/8 double-stator switched reluctance motor for washing machine application," in *Proc. 6th Power Electron., Drive Syst. Technol. Conf. (PEDSTC)*, Feb. 2015, pp. 168–172.

[6] E. Elhomdy, G. Li, J. Liu, S. Bukhari, and W.-P. Cao, "Design and experimental verification of a 72/48 switched reluctance motor for low-speed direct-drive mining applications," *Energies*, vol. 11, no. 1, p. 192, Jan. 2018.

[7] X. Sun, K. Diao, G. Lei, Y. Guo, and J. Zhu, "Study on segmented-rotor switched reluctance motors with different rotor pole numbers for BSG system of hybrid electric vehicles," *IEEE Trans. Veh. Technol.*, vol. 68, no. 6, pp. 5537–5547, Jun. 2019.

[8] V. Rallabandi, J. Wu, A. M. Cramer, D. M. Ionel, and P. Zhou, "Optimal design of outer rotor switched reluctance machines for direct drive rim applications," in *Proc. IEEE Energy Convers. Congr. Expo. (ECCE)*, Sep. 2018, pp. 6104–6109.

[9] R. Vandana, S. Nikam, and B. G. Fernandes, "High torque polyphase segmented switched reluctance motor with novel excitation strategy," *IET Electr. Power Appl.*, vol. 6, no. 7, pp. 375–384, Aug. 2012.
[10] G. Davarpanah and J. Faiz, "A novel structure of switched reluctance machine with higher mean torque and lower torque ripple," *IEEE Trans. Energy Convers.*, vol. 35, no. 4, pp. 1859–1867, Dec. 2020.
[11] J.-W. Ahn and D.-H. Lee, "Performance of passive boost switched reluctance converter for single-phase switched reluctance motor," *J. Electr. Eng. Technol.*, vol. 6, no. 4, pp. 505–512, Jul. 2011.
[12] W. Ding, S. Yang, and Y. Hu, "A novel boost converter for segmented-stator hybrid-excitation switched reluctance motor drive with high performance," in *Proc. IEEE Appl. Power Electron. Conf. Expo. (APEC)*, Mar. 2018, pp. 1223–1228.
[13] Y. Zhu, C. Yang, Y. Yuan, C. Zhao, and Z. Yan, "Development and analysis of a two-phase excitation switched reluctance motor with novel winding distribution used in electric vehicles," *J. Electr. Eng. Technol.*, vol. 13, no. 6, pp. 2364–2375, 2018.
[14] X. Deng, B. Mecrow, R. Martin, and S. Gadoue, "Effects of winding connection on performance of a six-phase switched reluctance machine," *IEEE Trans. Energy Convers.*, vol. 33, no. 1, pp. 166–178, Mar. 2018.
[15] S. Kocan, P. Rafajdus, P. Makys, and R. Bastovansky, "Design of high speed switched reluctance motor," in *Proc. Int. Conf. Expo. Electr. Power Eng. (EPE)*, Oct. 2018, pp. 0421–0426.
[16] I. Kioskeridis and C. Mademlis, "Optimal efficiency control of switched reluctance generators," *IEEE Trans. Power Electron.*, vol. 21, no. 4, pp. 1062–1071, Jul. 2006.
[17] A. Chiba, Y. Takano, M. Takeno, T. Imakawa, N. Hoshi, M. Takemoto, and S. Ogasawara, "Torque density and efficiency improvements of a switched reluctance motor without rare-earth material for hybrid vehicles," *IEEE Trans. Ind. Appl.*, vol. 47, no. 3, pp. 1240–1246, May/Jun. 2011.
[18] Q. Yu, B. Bilgin, and A. Emadi, "Loss and efficiency analysis of switched reluctance machines using a new calculation method," *IEEE Trans. Ind. Electron.*, vol. 62, no. 5, pp. 3072–3080, May 2015.
[19] Y. Xu, R. Zhong, L. Chen, and S. Lu, "Analytical method to optimise turn-on angle and turn-off angle for switched reluctance motor drives," *IET Electr. Power Appl.*, vol. 6, no. 9, pp. 593–603, 2012.
[20] H.-J. Chen and J.-Y. Li, "A simple turn-on and turn-off angles searching method for copper loss minimization of the switched reluctance motor," *COMPEL-Int. J. Comput. Math. Electr. Electron. Eng.*, vol. 36, no. 4, pp. 1059–1074, Jul. 2017.
[21] S. Kittiratsatcha, P. Kerdtuad, and C. Bunlaksananusorn, "Output power control using artificial neural network for switched reluctance generator," *Sensors Mater.*, vol. 33, no. 7, p. 2427, 2021.
[22] C. Ma and L. Qu, "Multiobjective optimization of switched reluctance motors based on design of experiments and particle swarm optimization," *IEEE Trans. Energy Convers.*, vol. 30, no. 3, pp. 1144–1153, Sep. 2015.
[23] W. Ding, H. Zhou, and Z. Yu, "Magnetic flux and iron loss estimation of a switched reluctance motor," *Electr. Mach. Control Appl.*, vol. 33, no. 6, pp. 11–17, 2006.

PENG YANG received the B.S. degree in mechanical engineering and the master's degree in mechatronics from Shanghai Jiao Tong University, Shanghai, China, in 2008 and 2011, respectively, where he is currently pursuing the Ph.D. degree in aeronautical and astronautical science and technology. He serves as a Senior Engineer at the Shanghai Aircraft Design and Research Institute, COMAC. His current research interests include aircraft landing gear, brake systems, and system integration.

WEI SHI was born in Nantong, Jiangsu, China, in 1996. He received the B.S. degree in electromechanical engineering and automation from Yangzhou University, Yangzhou, China, in 2018. He is currently pursuing the master's degree with the University of Shanghai for Science and Technology. His current research interest includes motor design and optimization based on multi-physics analysis.

YUE QIU received the master's degree in electrical engineering from Dalian Jiaotong University, Dalian, China, in 2015. He is currently working at CRRC Industrial Research Institute (Qingdao). His current research interests include motor design for high-speed railway and new generation of TSN-based train communication.

BINGCHU LI (Member, IEEE) received the B.S. degree in mechanical engineering from Central South University, Hunan, China, in 2008, and the Ph.D. degree in mechanical engineering from Shanghai Jiao Tong University, Shanghai, China, in 2019. He is currently an Assistant Professor with the University of Shanghai for Science and Technology. His current research interests include intelligent robotics, high reliable actuators, and electromechanical system design with emphasis on switched reluctance machines.

YI GAN received the Ph.D. degree in mechanical engineering from Tongji University, Shanghai, China, in 2004. From 2004 to 2006, he served as an Assistant Professor with the School of Mechanical Engineering, University of Shanghai for Science and Technology, where he served as an Associate Professor, from 2006 to 2017, and has been a Professor, since 2017. He is currently a Co-Researcher with the Faculty of Science and Engineering, Chuo University, Kyoto, Japan. His current research interests include intelligent mechatronics system design and intelligent manufacturing.